Fourier-transform infrared (FT-IR) spectroscopy analysis discriminates asymptomatic and symptomatic Norway spruce trees

Mukrimin, Mukrimin

2019-12

Mukrimin , M , Conrad , A O , Kovalchuk , A , Julkunen-Tiitto , R , Bonello , P & Asiegbu , F O 2019 , ' Fourier-transform infrared (FT-IR) spectroscopy analysis discriminates asymptomatic and symptomatic Norway spruce trees ' , Plant Science , vol. 289 , 110247 . https://doi.org/10.1016/j.p

http://hdl.handle.net/10138/308544
https://doi.org/10.1016/j.plantsci.2019.110247

Plant Science 289 (2019) 110247

Contents lists available at ScienceDirect

Plant Science

journal homepage: www.elsevier.com/locate/plantsci

Fourier-transform infrared (FT-IR) spectroscopy analysis discriminates asymptomatic and symptomatic Norway spruce trees

Mukrimin Mukrimin[a,b,1], Anna O. Conrad[c,1], Andriy Kovalchuk[a], Riitta Julkunen-Tiitto[d], Pierluigi Bonello[c], Fred O. Asiegbu[a,*]

[a] Department of Forest Sciences, Faculty of Agriculture and Forestry, University of Helsinki, Latokartanonkaari 7, P.O. Box 27, 00014, Helsinki, Finland
[b] Department of Forestry, Faculty of Forestry, Hasanuddin University, Jln. Perintis Kemerdekaan Km. 10, 90245, Makassar, Indonesia
[c] Department of Plant Pathology, The Ohio State University, 2021 Coffey Road, Columbus, OH, 43210, USA
[d] Department of Environmental and Biological Sciences, Joensuu Campus, University of Eastern Finland (UEF), P.O. Box 111, FI-80101, Joensuu, Finland

ARTICLE INFO

Keywords:
Norway spruce
Heterobasidion
FT-IR spectroscopy
Chemometric analysis
SIMCA
PLSR
Mid-IR spectra

ABSTRACT

Conifer trees, including Norway spruce, are threatened by fungi of the *Heterobasidion annosum* species complex, which severely affect timber quality and cause economic losses to forest owners. The timely detection of infected trees is complicated, as the pathogen resides within the heartwood and sapwood of infected trees. The presence of the disease and the extent of the wood decay often becomes evident only after tree felling. Fourier-transform infrared (FT-IR) spectroscopy is a potential method for non-destructive sample analysis that may be useful for identifying infected trees in this pathosystem. We performed FT-IR analysis of 18 phloem, 18 xylem, and 18 needle samples from asymptomatic and symptomatic Norway spruce trees. FT-IR spectra from 1066 – 912 cm^{-1} could be used to distinguish phloem, xylem, and needle tissue extracts. FT-IR spectra collected from xylem and needle extracts could also be used to discriminate between asymptomatic and symptomatic trees using spectral bands from 1657 – 994 cm^{-1} and 1104 – 994 cm^{-1}, respectively. A partial least squares regression model predicted the concentration of condensed tannins, a defense-related compound, in phloem of asymptomatic and symptomatic trees. This work is the first to show that FT-IR spectroscopy can be used for the identification of Norway spruce trees naturally infected with *Heterobasidion* spp.

1. Introduction

Conifers, including Norway spruce (*Picea abies*) and Scots pine (*Pinus sylvestris*), are a major source of wood products for the Finnish forest industry, an important sector of the Finnish economy. In 2015, this sector contributed approximately 11.6 billion euros of exported product, which accounted for around 5% of Finnish gross domestic product, and approximately 22% of Finnish exports [1]. Nevertheless, this natural resource is threatened by arthropod pests and pathogens, including fungi of the *Heterobasidion annosum* species complex, which causes root and butt rot diseases [2,3]. The pathogen is one of the most serious problems for Finnish forests as well as northern boreal conifer forests with annual economic losses estimated at 50 and 800 million euros for Finnish forest and European forest owners, respectively [4–6].

The *H. annosum* species complex, based on morphological features, ecology, and molecular analysis, consists of three European species: *H. annosum sensu stricto*, *H. parviporum* and *H. abietinum* with Scots pine, Norway spruce and silver fir as preferred hosts, respectively, and two North American species: *H. irregulare* (attacking species of pine, juniper, and incense cedar) and *H. occidentale* (with broad host range, including species of fir, spruce, hemlock, Douglas-fir (*Pseudotsuga menziesii*) and *Sequoiadendron giganteum*) [4,7]. *Heterobasidion annosum* has a unique life-style, as it can live both as a saprotroph (on dead wood tissues) and as a necrotroph (by killing living cells of the host trees) [7–10]. In Finnish forests alone, about 15% of the Norway spruce trees harvested are rotted due to infection by *H. parviporum*. The proportion of decay by volume caused by *Heterobasidion* is about 47–90% of the total rot in Norway spruce [11].

Unlike many other forest tree pathogens, the symptoms of infection by *Heterobasidion* spp. are not overtly manifested and often remain obscure even for experienced forest pathologists. In Norway spruce, the pathogen resides within heartwood and sapwood, causing a formation of a decay column within the trunk, but the infection may remain unnoticed for years. In the absence of visible fruiting bodies of the

* Corresponding author.
E-mail address: fred.asiegbu@helsinki.fi (F.O. Asiegbu).
[1] Contributed equally as first authors.

https://doi.org/10.1016/j.plantsci.2019.110247
Received 9 May 2019; Received in revised form 28 August 2019; Accepted 30 August 2019
Available online 03 September 2019

pathogen and readily observable symptoms, the extent of the decay often becomes evident only after tree felling, either during thinning or harvesting. Therefore, the cryptic nature of *Heterobasidion* infection prevents timely detection of infected trees and contributes to the pathogen damage.

Conifers have constitutive and induced defense systems to protect against pathogen invasion. Some of the inherent chemical defenses of conifer tissues include the ability to synthesize and secrete compounds (*e.g.*, terpenes, flavonoids, stilbenes, lignans, *etc*.) that immobilize or are toxic to invading organisms, and bolster trees' defense against pathogens like *Heterobasidion* [12]. The pathogen can also be managed by a combination of silvicultural methods (*e.g.*, stump removal, thinning, and pruning), chemical control (*e.g.*, urea and borates), and by a biological control agent (*e.g.*, *Phlebiopsis gigantea*). Unfortunately, these methods do not offer 100% protection [13]. In fact, conifer trees with natural resistance against the pathogen are desired; hence, a primary objective of our work is to figure out an alternative technique for identifying genetic or chemical biomarkers of resistance.

Currently available approaches for screening and phenotyping trees for disease resistance based on both natural and artificial infection are not optimal, effective, or efficient. Currently available approaches are laborious and time-consuming, and depend on the trees' age and size [14–17]. An ideal approach would be rapid, accurate, cost-effective, and should have the potential to be adapted for high-throughput screening or phenotyping under field conditions [18,19].

One such approach is chemical phenotyping (chemotyping or chemical fingerprinting). This technique enables profiling of a wide spectrum of plant-derived chemicals, which is more advantageous in comparison with traditional approaches that focus either on a single chemical compound or on a limited number of compounds. In addition, chemical fingerprinting has the potential utility for 1) reducing the space and time needed to inoculate progeny/assess disease resistance; 2) identifying biomarkers of disease resistance; and 3) developing and validating predictive models [17]. Fourier-transform infrared (FT-IR) spectroscopy is a commonly used vibrational spectroscopy method, which can be used to produce chemical fingerprints of solid, liquid, or gaseous samples. The technique can be more effective and efficient than other traditional approaches [19,20]. It has promising results in applications involving forest trees, and is able to successfully predict tree resistance prior to infection [21]. Hence, the use of FT-IR spectroscopy should provide additional insights in the study of the *Heterobasidion*-conifer pathosystem.

Previous studies, using the same cohort of 'asymptomatic' (without visible decay symptoms) and 'symptomatic' (with well-defined decay symptoms) Norway spruce trees, showed that these trees are naturally infected with *Heterobasidion* spp. [22,23] and have different levels of host transcripts, phenolics, and terpenoids [24].

We hypothesized that FT-IR spectroscopy would allow us to discriminate both between tissues and between symptomatic and asymptomatic trees. We also explored the possibility of using needle samples for this purpose, as this would allow for rapid screening without the need for invasive sampling of woody tissues. Additionally, we examined whether the observed differences in FT-IR spectra of sampled trees correlate with the concentration of selected chemicals with a potential role in chemical defense.

2. Materials and methods

2.1. Sample collection from asymptomatic and symptomatic trees

Norway spruce xylem (sapwood/heartwood) and phloem (inner bark) and needle tissues were sampled in May 2016 from three different plots in forest sites of Mäntsälä in the Uusimaa region, Southern Finland (60°44′51″-60°45′15″N, 25°13′17″-25°15′34″E). Further information on sampling plots can be found in Kovalchuk et al. and Ren et al. [22,23]. In brief, sampling plots were located within a managed Norway spruce forest, with tree age of ca. 55–60 years and approximately 15–20 meter in height at the time of sampling. Xylem (sapwood/heartwood) and phloem (inner bark) and needle tissues were collected from the three plots. Xylem and phloem were taken at the stump level, and second year needles were sampled from the top crown. Xylem samples used for analysis were cross sections containing both early and late woods, whereas phloem samples were mechanically separated by removing the outer bark. Sampling was conducted simultaneously with tree harvesting. Samples were collected within a few minutes after respective trees were felled, put in dry ice, and then stored in a –80° C freezer until further analysis.

The sampled trees were classified as asymptomatic or symptomatic depending on the presence of visible wood decay symptoms in the xylem (heartwood and sapwood) at the stump level. Asymptomatic trees had no visually detectable symptoms of wood decay, whereas symptomatic trees were characterized by the presence of clear symptoms of decay. The trees were naturally infected by *Heterobasidion* spp., and no artificial inoculations were performed. Presence of *Heterobasidion* in decayed trees was confirmed by molecular identification [22]. Sampled xylem and phloem tissues were subjected to chemical analysis, and the content of phenolic compounds was determined [23,24].

2.2. FT-IR analysis

The frozen samples, 200 mg ± 1 mg, were finely ground to powder by an IKA® A11 basic mill (IKA-Werke GmbH & Co. KG, Germany) in liquid N_2. Samples were extracted using 70% acetone and chloroform, and cleaned-up according to the method of Wrolstad et al. and Villari et al. [21,25]. Extracts (200 µL) were dried completely in a SpeedVac (Thermo Fisher Scientific, MA, USA), and shipped on dry ice to The Ohio State University, Columbus, OH, USA for subsequent FT-IR analysis. Prior to analysis, dried extracts were re-suspended in 20 µL methanol to a final concentration (10x). A single-bounce attenuated total reflectance (ATR) accessory on a portable Cary 630 FT-IR spectrometer (Agilent Technologies Inc., Santa Clara, CA, USA) was used to analyze 5 µl of purified and concentrated methanol extracts. Samples were allowed to sit for 5 min to allow the evaporation of methanol, which interferes with the FT-IR spectrum [20].

2.3. Determination of condensed tannins

The concentration of condensed tannins in phloem of the sampled trees was estimated using the acid butanol assay as described previously [26,27].

2.4. Statistical analysis

FT-IR data were analyzed using the chemometrics software Pirouette version 4.5 (Infometrix Inc., Woodville, WA, USA). To discriminate among tree tissues or needles and between asymptomatic and symptomatic trees, soft independent modeling of class analogy (SIMCA) was performed. Partial least squares regression (PLSR) was also used to estimate the concentration of condensed tannin based on FT-IR spectra [17]. SIMCA analysis is a classification technique based on similarity of regions and a technique that is used for supervised classification by identifying areas of the FT-IR spectrum that are most useful for discriminating between groups [28].

3. Results and discussion

3.1. Phloem, xylem and needle tissues comparison

This study represents the first report of FT-IR analysis performed on Norway spruce in association with *Heterobasidion* sp. infection. To determine if FT-IR spectroscopy combined with chemometric analysis can

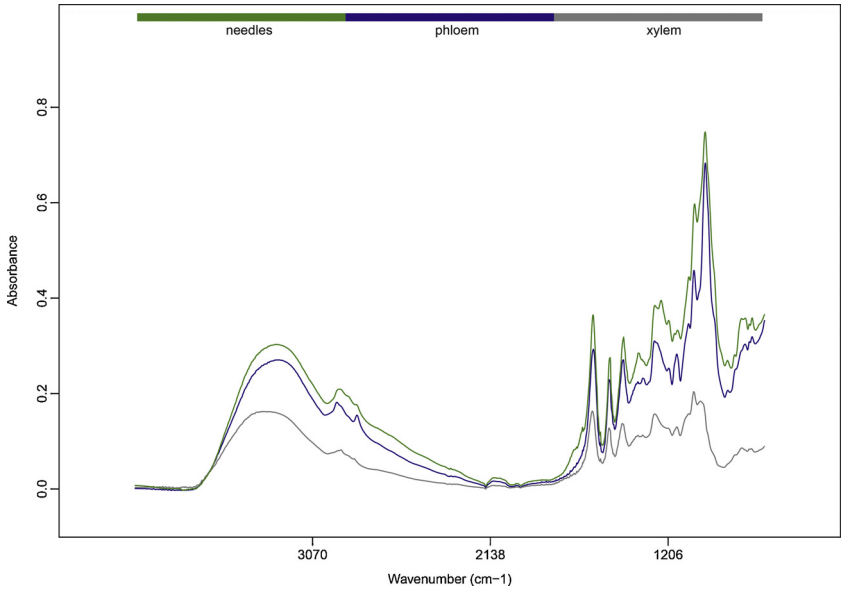

Fig. 1. Average untransformed spectra for each tissue from 4000 – 700 cm^{-1} for Norway spruce phloem (blue, N = 36), xylem (grey, N = 30), and needles (green, N = 36). Three xylem biological replicates (six total technical replicates) were trimmed due to absorbance values close to zero.

distinguish between phloem, xylem, and needle extracts, SIMCA was performed. One-hundred eight total spectra (including two technical replicates per biological replicate) from the mid-IR region (4000 – 700 cm^{-1}) were collected from 54 biological samples (N_{phloem} = 18, N_{xylem} = 18, and $N_{needles}$ = 18) (Fig. 1). Technical replicates were analyzed separately in the chemometric analyses.

Prior to conducting the SIMCA analysis, data were randomly split into training and testing data sets using a random number generator. The training set included 70% of the samples (N_{train} = 75), while the testing set included 30% of samples (N_{test} = 33). The training data set was used to build the SIMCA model, and the testing data set was used to evaluate the performance of model. Prior to SIMCA analysis, each data set was cleaned so as to exclude any samples with absorbance values close to zero. From each data set, three technical replicates meeting this criterion were excluded. Second derivative (25 points) and smoothed (25 points) spectra between 1066 – 912 cm^{-1} (Fig. 2) can be used to distinguish between phloem, xylem, and needle extracts using a SIMCA with 2-factors for each class (Fig. 3).

The training model included 88% (N = 75) of technical replicates, with close to zero absorbance replicates excluded. Of those samples (N = 66), 97% were correctly classified by the model, while 3% were misclassified. The interclass distance between tissues varied, but the greatest distance was between phloem and xylem (Table 1). Interclass distance is used to assess the separation between groups in the SIMCA model, and optimize SIMCA models [29]. The spectral band with the highest discriminating power was 1008 cm^{-1} (discriminating power = 968) associated with C—O stretching of starch [30]. Three replicates were excluded from the testing data set (9%, N = 33) before samples were analyzed with the SIMCA model generated from the training data set. Eighty-three percent of testing data set samples were correctly classified, while 17% were misclassified or had no match (N = 30). The results showed that phloem, xylem, and needle tissues can be separated based on their FT-IR spectrum.

These results reflect differences in the chemical composition of those tissues or needles. An earlier study also revealed that the content of metabolites were different between the phloem and xylem of mature Scots pine trees and their contents of low molecular weight (MW) carbohydrates, amino acids, organic acids, and phenolic compounds were significantly different between phloem and xylem [31]. Another study demonstrated that *Pinus radiata* two year old seedlings differed significantly in their content of two major secondary chemicals, namely resin and polyphenolics, among stem phloem, stem xylem, and needles

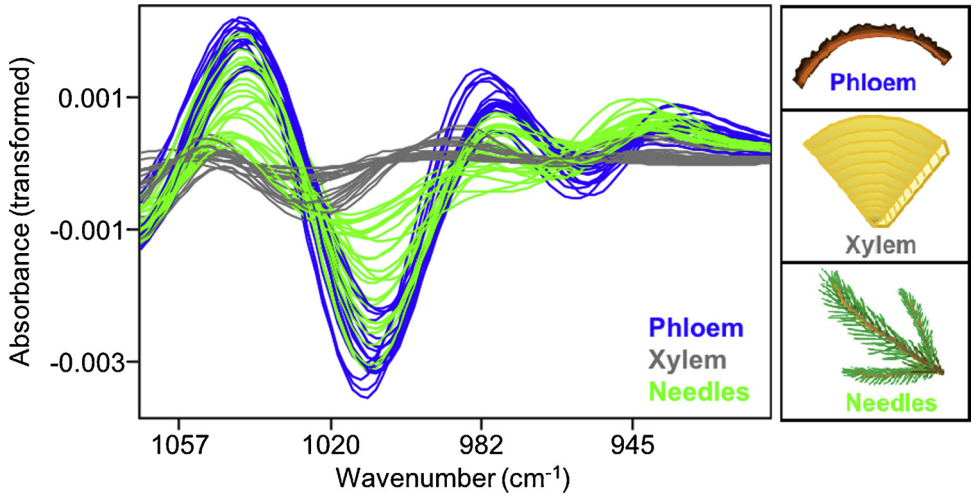

Fig. 2. Second derivative and smoothed spectra between 1066 – 912 cm^{-1} for phloem (blue), xylem (grey), and needles (green).

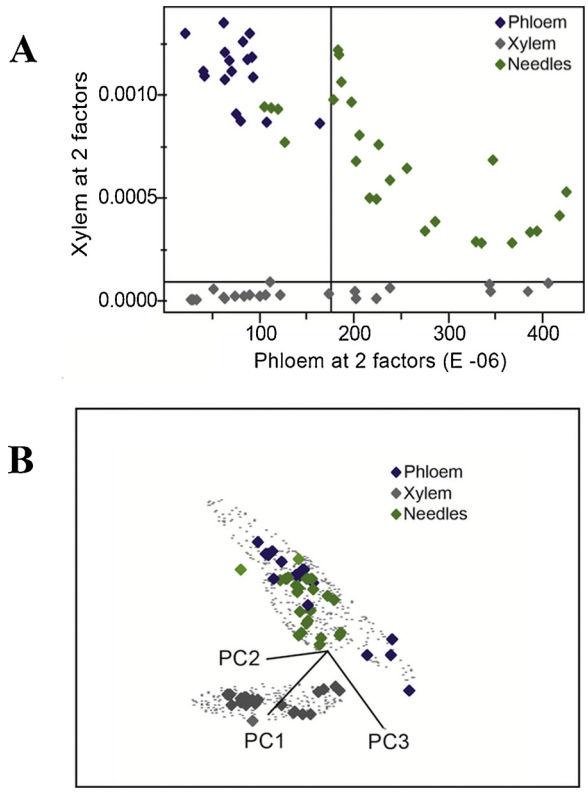

Fig. 3. (A) Class distances (Cooman's) plot showing the dimension-free distance from a sample to a given class, phloem (x-axis) or xylem (y-axis) based on a SIMCA analysis of a training data set with 2-factors for each class. Vertical and horizontal black lines indicate critical sample residual thresholds. (B) 3-D class projection plot from SIMCA analysis. Grey dots indicate the 95% confidence interval for each class. For all plots, blue diamonds: phloem, grey diamonds: xylem, and green diamonds: needles. (N = 66).

Table 1
Interclass distances from SIMCA analysis of phloem, xylem, and needle extracts.

Comparison	Interclass distance
phloem *vs.* xylem	11.14
phloem *vs.* needles	1.65
xylem *vs.* needles	4.84

[32].

3.2. Comparison between asymptomatic and symptomatic trees

We conducted a SIMCA analysis to determine if FT-IR spectroscopy combined with chemometric analysis can distinguish between extracts of the tissues or organ collected from asymptomatic and symptomatic trees. Since pronounced differences were observed in the spectral patterns of phloem, xylem, and needle extracts, we compared samples from asymptomatic and symptomatic trees for each phloem, xylem, and needles separately. For each tissue, spectra were collected from 18 biological replicates. Two technical replicates were collected and analyzed separately for each biological replicate (N_{phloem} = 36, N_{xylem} = 36, and $N_{needles}$ = 36).

3.2.1. Phloem

We were unable to distinguish between phloem extracts from asymptomatic and symptomatic trees using SIMCA analysis. However, a PLSR model was able to predict the concentration of condensed tannins in phloem from both asymptomatic and symptomatic trees (see Section 3.3. below). Future analysis of larger numbers of asymptomatic and symptomatic trees would help determine if there are spectral differences in phloem extracts, and if these differences can be used to discriminate between groups using a SIMCA approach.

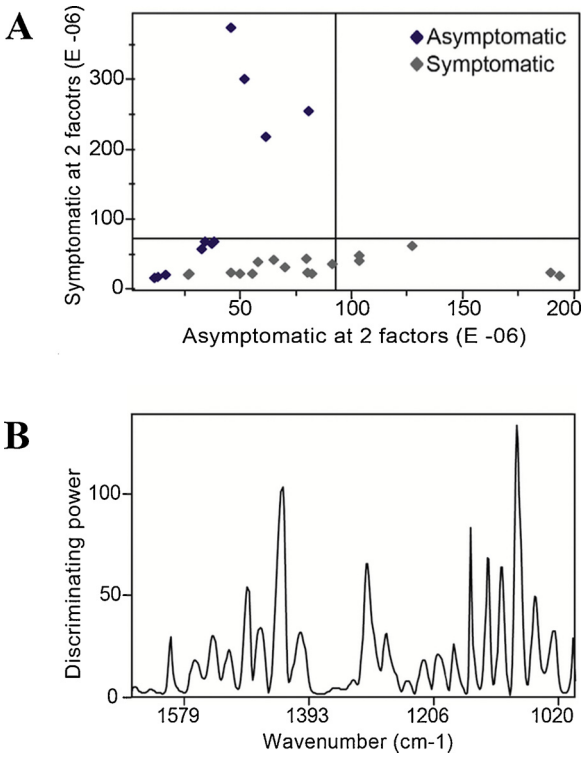

Fig. 4. (A) Class distances (Cooman's) plot for xylem showing the dimension-free distance from a sample to a given class, asymptomatic (x-axis) or symptomatic (y-axis), based on SIMCA analysis with 2-factors for each class (N = 29). Vertical and horizontal black lines indicate critical sample residual thresholds. (B) Discriminating power plot showing the discriminating power of individual spectral bands from 1657 – 994 cm^{-1}.

3.2.2. Xylem

Second derivative (25 points) and smoothed (25 points) spectra from 1657 – 994 cm^{-1} can be used to discriminate between asymptomatic and symptomatic trees using xylem extracts (Fig. 4). Eighty-one percent (N = 36) of samples were included in the SIMCA model with two factors for each class, and of those samples 100% were correctly classified (N = 29). The spectral bands with the highest discriminating power were 1432 cm^{-1} (discriminating power = 104) and 1081 cm^{-1} (discriminating power = 134) (Fig. 4B). The interclass distance between asymptomatic and symptomatic trees was 2.69, indicating that xylem extracts from asymptomatic and symptomatic trees could be reliably distinguished. The spectral region from 1657 – 994 cm^{-1} corresponded primarily to carbohydrate (C—O), carbonyl (C═O), and benzene (C═C) group-stretching vibrations [20], while the two peaks showing the highest discriminating power were associated with lignin and carbohydrates (1432 cm^{-1}), and cellulose and hemicellulose (1081 cm^{-1}) [33]. Similar results have been observed by Pandey and Pitman [34], where beech (*Fagus sylvatica* L.) sapwood produced many well-defined peaks in the spectral regions of 1596, 1505, 1330, 1230 and 1122 cm^{-1}, whereas in Scots pine (*Pinus sylvestris* L.) sapwood generated well-defined peaks at 1596, 1511, 1268 and 1220 cm^{-1}, which were associated with lignin. Another study performed by Cardinali et al. [35] found that FT-IR can distinguish between healthy, symptomatic, and asymptomatic leaves from adult trees of sweet orange (*Citrus sinensis* L. Osbeck) infected by the pathogen *Xylella fastidiosa* and *Candidatus* Liberibacter spp., and that spectral bands from

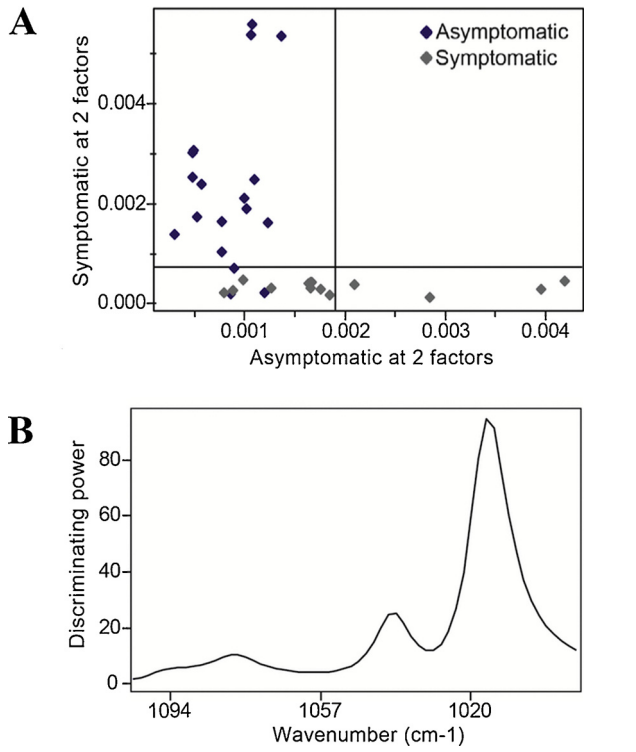

Fig. 5. (A) Class distances (Cooman's) plot for needles showing the dimension-free distance from a sample to a given class, asymptomatic (x-axis) or symptomatic (y-axis), based on SIMCA analysis with 2-factors for each class (N = 32). Vertical and horizontal black lines indicate critical sample residual thresholds. (B) Discriminating power plot showing the discriminating power of individual spectral bands from 1104 – 994 cm^{-1}.

1175 – 900 cm^{-1} were associated with the absorption of starch. Villari et al. [21] also demonstrated that European ash (*Fraxinus excelsior*) trees resistant and susceptible to ash dieback disease could be distinguished using SIMCA together with FT-IR spectroscopy analysis of phenolic extracts from uninfected bark tissue.

3.2.3. Needles

First derivative (25 points) and smoothed (25 points) spectra from 1104 – 994 cm^{-1} can be used to discriminate between asymptomatic and symptomatic trees using needle extracts (Fig. 5). This spectral region (1104 – 994 cm^{-1}) corresponds primarily to carbohydrate (C—O) group-stretching vibrations [20]. The SIMCA model included 89% (N = 36) of samples with two factors for each class, and of those samples (*N* = 32) 91% were correctly classified, while 9% were misclassified. The spectral band with the highest discriminating power was 1016 cm^{-1} (discriminating power = 95) (Fig. 5B). The interclass distance between asymptomatic and symptomatic trees was 2.75, indicating that the model was capable of separating asymptomatic and symptomatic trees based on needle extracts.

Needle extracts from symptomatic and asymptomatic trees could be discriminated in the present study. High discriminating power was associated with the band at 1016 cm^{-1}, which is associated with carbohydrate (C—O) group-stretching vibrations of cellulose and hemicellulose [33]. Bands in this region have also been used to discriminate between naturally decayed and non-decayed cypress (*Cupressus sempervirens* L.) woods using FT-IR spectroscopy [36]. In Abdallah et al. [36], the non-decayed cypress wood spectra from 1800 – 600 cm^{-1} were assigned to cellulose, hemicellulose, and lignin moieties. The spectral regions of decayed cypress wood were from 1735 – 898 cm^{-1} and were associated with carbohydrate bands [36]. They found that the chemical structure of naturally decayed wood was significantly different from the non-decayed wood, as indicated by decreased band intensity, and probably due to fungal infection and aging factors [36]. Another study [37], revealed that the FT-IR spectra of non-decayed hornbeam (*Carpinus betulus* L.) wood and hornbeam wood decayed by *Trametes versicolor* (white rot fungus) showed marked differences within the region of 1800 – 500 cm^{-1}. Hence, FT-IR spectroscopy has been proven as a useful tool to follow changes in both the chemical composition and biophysics of fungal-decayed wood [38].

In the present study, we identified spectral regions (xylem at 1657 – 994 cm^{-1} and needles at 1104 – 994 cm^{-1}) that can be used to discriminate between samples from asymptomatic and symptomatic trees. The observed spectral differences likely reflect differences in chemical composition, caused by fungal infection of tree root and/or butt. This is consistent with the previous results of our chemical analysis, which demonstrated accumulation of lignans and neolignans in the xylem of symptomatic trees [24]. Conifers, including Norway spruce, have both induced and constitutive defenses against fungi and insects, including the bark of Norway spruce, which is often the first layer of defense [39]. When trees respond to an infection, their induced defenses are activated, producing enzymes and secondary metabolites, such as flavonoids, lignans, other low MW phenols, stilbenes, and terpenes [40–42]. In addition, wood properties, *e.g.*, presence of extractives, may affect the rate of fungal spread within trees [36]. This is consistent with our results, which found that FT-IR spectra could be used to differentiate between symptomatic and asymptomatic trees. Furthermore, the fact that we were able to differentiate between symptomatic and asymptomatic trees using needle extracts, suggests that systemic chemical changes are occurring in infected trees.

3.3. Predicting the concentration of condensed tannin in phloem

Tannins, which are commonly produced by trees, are polymeric polyphenolic compounds that can bind proteins, are oxidatively active, and also play a very important role in plant defense against arthropod pests and pathogens [43]. Tannins can also chelate metals, in particular iron, which is a common antimicrobial mechanism involved in microbial interactions [44,45]. Hence, we assessed whether or not the concentration of a defense-related tannins can be estimated based on the FT-IR spectrum.

A six-factor PLSR model with leave-one-out cross-validation was used to predict the concentration of condensed tannin (mg g^{-1} DW) in phloem using transformed (second derivative, 25 points, and normalized) spectra from 1680 – 1279 cm^{-1} (N = 25, with one technical replicate trimmed based on preliminary analysis) (Fig. 6). This is not the

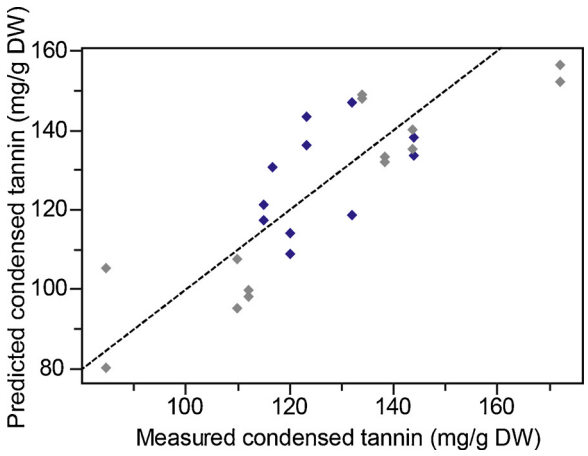

Fig. 6. A six-factor PLSR model can estimate the concentration of condensed tannin (mg g^{-1} DW) in phloem based on transformed spectra from 1680 – 1279 cm^{-1}, with 99.9% of the variance explained, a standard error of cross-validation (SECV) of 12.2, and a correlation coefficient of cross-validation (rVal) of 0.82. Blue: asymptomatic trees; grey: symptomatic trees.

first time that plant-produced compounds have been estimated using spectra. A previous study [46] showed that PLSR could be used to predict the total lignin content of Norway spruce wood, while a different study [47] used PLSR to predict lignin and energy contents in hybrid poplars (*Populus trichocarpa* × *P. deltoides*).

Leong et al. [48] has reviewed several tools for the detection of decay in standing trees, *e.g.*, infrared radiation emissivity, ultrasonic frequency, electrical resistivity, electromagnetic wave permittivity, *etc*. However, the methods proposed by these authors are most suitable for urban trees that can constitute a hazard, but perhaps less feasible in plantation and commercial forestry settings. An ideal approach suitable for plantation and commercial forestry would be a technique that is rapid, accurate, cost-effective, and has the potential to be adapted for high-throughput screening or phenotyping under these conditions. The feasibility of using FT-IR spectroscopy in plantation and commercial forestry settings deserves to be explored and merits further investigation. Furthermore, a long term objective of our work is to determine an alternative technique for identifying genetic or chemical biomarkers that can be deployed for resistance breeding against *Heterobasidion* root rot.

In conclusion, the present study is the first report highlighting the use of FT-IR spectroscopy as a tool for discriminating between asymptomatic and symptomatic Norway spruce trees infected by *Heterobasidion* sp. These promising results show that even needle extracts can be used to differentiate between symptomatic and asymptomatic trees. Nevertheless, further study is needed to determine the robustness of this tool in this pathosystem, and to validate the results of the present study. However, if validated, FT-IR combined with chemometrics may be a useful, relatively non-destructive screening tool for disease resistance-breeding programs for trees.

Author contributions

FOA, MM, AK, PB, and AC designed the experiment. MM and AK collected samples in the field. MM processed and extracted the samples. MM and AC performed FT-IR analyses and chemometric modeling. RJT analyzed the phenolic compounds. MM and AC analyzed the data. MM, AC, and AK prepared the manuscript draft. All authors discussed results, and read and approved the final version of the manuscript.

Declaration of Competing Interest

The authors declare that this article has no conflicts of interest.

Acknowledgements

This study was supported by funding from the Academy of Finland (Grant no. 307580 to FOA). We acknowledge the Doctoral School in Environmental, Food and Biological Sciences (YEB), University of Helsinki, Finland for supporting MM's visiting scholar program at The Ohio State University, USA. The Ministry of Research, Technology, and Higher Education (RISTEKDIKTI) of the Republic of Indonesia is acknowledged for scholarship to MM. We thank Dr. Risto Kasanen for help in field sampling, Marie F. Laborde and Caleb Mathias for help in preparing samples and performing FT-IR spectroscopy analysis, and Dr. Luis Rodriguez-Saona for access to the FT-IR spectrometer.

References

[1] E-yearbook Of Food and Natural Resource Statistics, E-yearbook of Food and Natural Resource Statistics for 2016: Statistical Facts on Agriculture, Forestry, Fisheries and Hunting in Finland, (2017), p. 84 http://urn.fi/URN:ISBN:978-952-326-407-6.

[2] M. Mukrimin, A. Kovalchuk, L.G. Neves, E. Jaber, M. Haapanen, M. Kirst, F.O. Asiegbu, Genome-wide exon-capture approach identifies genetic variants of Norway spruce genes associated with susceptibility to *Heterobasidion parviporum* infection, Front. Plant Sci. 9 (2018) 1–13, https://doi.org/10.3389/fpls.2018.00793.

[3] S. Keriö, S.M. Niemi, M. Haapanen, G. Daniel, F.O. Asiegbu, Infection of Picea abies clones with a homokaryotic isolate of *Heterobasidion parviporum* under field conditions, Can. J. For. Res. 45 (2014) 227–235, https://doi.org/10.1139/cjfr-2014-0247.

[4] F.O. Asiegbu, A. Adomas, J. Stenlid, Conifer root and butt rot caused by *Heterobasidion annosum* (Fr.) Bref. s.l, Mol. Plant Pathol. 6 (2005) 395–409, https://doi.org/10.1111/j.1364-3703.2005.00295.x.

[5] T. Piri, L. Hamberg, Persistence and infectivity of *Heterobasidion parviporum* in Norway spruce root residuals following stump harvesting, For. Ecol. Manage. 353 (2015) 49–58, https://doi.org/10.1016/j.foreco.2015.05.012.

[6] E. Terhonen, H. Sun, M. Buée, R. Kasanen, L. Paulin, F.O. Asiegbu, Effects of the use of biocontrol agent (*Phlebiopsis gigantea*) on fungal communities on the surface of Picea abies stumps, For. Ecol. Manage. 310 (2013) 428–433, https://doi.org/10.1016/j.foreco.2013.08.044.

[7] M. Garbelotto, P. Gonthier, Biology, epidemiology, and control of *Heterobasidion* species worldwide, Annu. Rev. Phytopathol. 51 (2013) 39–59, https://doi.org/10.1146/annurev-phyto-082712-102225.

[8] Hongxin Chen, *Heterobasidion annosum* sensu stricto pathogenesis: Bioinformatic and Functional Study of Cerato-platanin Family Proteins, PhD Thesis, University of Helsinki, 2015 ISSN 2342-3161 (Print); ISBN 978-951-51-1631-4 (paperback); ISBN 978-951-51-1632-1 (PDF) https://helda.helsinki.fi/handle/10138/157223.

[9] H. Sun, L. Paulin, E. Alatalo, F.O. Asiegbu, Response of living tissues of *Pinus sylvestris* to the saprotrophic biocontrol fungus *Phlebiopsis gigantea*, Tree Physiol. 31 (2011) 438–451, https://doi.org/10.1093/treephys/tpr027.

[10] Z. Zeng, H. Sun, E.J. Vainio, T. Raffaello, A. Kovalchuk, E. Morin, S. Duplessis, F.O. Asiegbu, Intraspecific comparative genomics of isolates of the Norway spruce pathogen (*Heterobasidion parviporum*) and identification of its potential virulence factors, BMC Genomics 19 (2018) 1–21, https://doi.org/10.1186/s12864-018-4610-4.

[11] U. Mattila, T. Nuutinen, Assessing the incidence of butt rot in Norway spruce in southern Finland, Silva Fenn. 41 (2007) 29–43, https://doi.org/10.14214/sf.473.

[12] Y.P. Rodriguez, L. Morales, S. Willfor, P. Pulkkinen, H. Peltola, A. Pappinen, Wood decay caused by *Heterobasidion parviporum* in juvenile wood specimens from normal- and narrow-crowned Norway spruce, Scand. J. For. Res. 28 (2013) 331–339, https://doi.org/10.1080/02827581.2012.746387.

[13] T. Möykkynen, J. Miina, T. Pukkala, K. Von Weissenberg, Modelling the spread of butt rot in a *Picea abies* stand in Finland to evaluate the profitability of stump protection against *Heterobasidion annosum*, For. Ecol. Manage. 106 (1998) 247–257, https://doi.org/10.1016/S0378-1127(97)00317-4.

[14] F. Isik, Genomic selection in forest tree breeding: the concept and an outlook to the future, New For. 45 (2014) 379–401, https://doi.org/10.1007/s11056-014-9422-z.

[15] F.A. Aravanopoulos, I. Ganopoulos, A. Tsaftaris, Population and Conservation Genomics in Forest and Fruit Trees, Elsevier Ltd, 2015, https://doi.org/10.1016/bs.abr.2015.04.001.

[16] D.B. Neale, A. Kremer, Forest tree genomics: growing resources and applications, Nat. Rev. Genet. 12 (2011) 111–122, https://doi.org/10.1038/nrg2931.

[17] A.O. Conrad, P. Bonello, Application of infrared and raman spectroscopy for the identification of disease resistant trees, Front. Plant Sci. 6 (2016) 1–8, https://doi.org/10.3389/fpls.2015.01152.

[18] Y. Yang, Y. Zhang, C. He, M. Xie, H. Luo, Y. Wang, J. Zhang, Rapid screen of aflatoxin-contaminated peanut oil using Fourier transform infrared spectroscopy combined with multivariate decision tree, Int. J. Food Sci. Technol. 53 (2018) 2386–2393, https://doi.org/10.1111/ijfs.13831.

[19] H.J. Song, Y.D. Kim, M.J. Jeong, M.S. Ahn, S.W. Kim, J.R. Liu, M.S. Choi, Rapid selection of theanine-rich green tea (*Camellia sinensis* L.) trees and metabolites profiling by Fourier transform near-infrared (FT-IR) spectroscopy, Plant Biotechnol. Rep. 9 (2015) 55–65, https://doi.org/10.1007/s11816-015-0344-9.

[20] A.O. Conrad, L.E. Rodriguez-Saona, B.A. McPherson, D.L. Wood, P. Bonello, Identification of *Quercus agrifolia* (coast live oak) resistant to the invasive pathogen Phytophthora ramorum in native stands using Fourier-transform infrared (FT-IR) spectroscopy, Front. Plant Sci. 5 (2014) 1–9, https://doi.org/10.3389/fpls.2014.00521.

[21] C. Villari, A. Dowkiw, R. Enderle, M. Ghasemkhani, T. Kirisits, E.D. Kjær, D. Marčiulynienė, L.V. McKinney, B. Metzler, F. Muñoz, L.R. Nielsen, A. Pliūra, L.-G. Stener, V. Suchockas, L. Rodriguez-Saona, P. Bonello, M. Cleary, Advanced spectroscopy-based phenotyping offers a potential solution to the ash dieback epidemic, Sci. Rep. 8 (2018) 17448, https://doi.org/10.1038/s41598-018-35770-0.

[22] A. Kovalchuk, M. Mukrimin, Z. Zeng, T. Raffaello, M. Liu, R. Kasanen, H. Sun, F.O. Asiegbu, Mycobiome analysis of asymptomatic and symptomatic Norway spruce trees naturally infected by the conifer pathogens *Heterobasidion* spp, Environ. Microbiol. Rep. 00 (2018) 1–10, https://doi.org/10.1111/1758-2229.12654.

[23] F. Ren, A. Kovalchuk, M. Mukrimin, M. Liu, Z. Zeng, R.P. Ghimire, M. Kivimäenpää, J.K. Holopainen, H. Sun, F.O. Asiegbu, Tissue microbiome of Norway spruce affected by Heterobasidion-induced wood decay, Microb. Ecol. (2018) 1–11.

[24] A. Kovalchuk, Z. Zeng, R.P. Ghimire, M. Kivimäenpää, T. Raffaello, M. Liu, M. Mukrimin, R. Kasanen, H. Sun, R. Julkunen-tiitto, J.K. Holopainen, F.O. Asiegbu, Dual RNA-seq analysis provides new insights into interactions between Norway spruce and necrotrophic pathogen *Heterobasidion annosums*. l, BMC Plant Biol. 19 (2019) 1–17.

[25] R.E. Wrolstad, T.E. Acree, E.A. Decker, D.S. Penner, M.H. Reid, S.J. Schwartz, C.F. Shoemaker, D. Smith, P. Sporns, Handbook of Food Analytical Chemistry: Pigments, Colorants, Flavors, Texture, and Bioactive Food Components, 1st ed., John Wiley and Sons, Inc, New York, 2005 doi:0-471-72187-5.

[26] V. Virjamo, R. Julkunen-Tiitto, Shoot development of Norway spruce (*Picea abies*) involves changes in piperidine alkaloids and condensed tannins, Trees - Struct.

Funct. 28 (2014) 427–437, https://doi.org/10.1007/s00468-013-0960-3.
[27] A.E. Hagerman, Acid Butanol Assay for Proanthocyanidins, Department of Chemistry & Biochemistry, Miami University, Oxford, OH, 2002 45056 Available at http://www.users.muohio.edu/ hagermae/, 2002. doi:S0143-4004(06)00059-2 [pii]\r10.1016/j.placenta.2006.03.006.
[28] Pirouette Multivariate Data Analysis Software, I. Inc., 2011, http://www.infometrix.com/.
[29] H. Tsugawa, Y. Tsujimoto, M. Arita, T. Bamba, E. Fukusaki, GC/MS based metabolomics: development of a data mining system for metabolite identification by using soft independent modeling of class analogy (SIMCA), BMC Bioinform. 12 (2011) 131, https://doi.org/10.1186/1471-2105-12-131.
[30] J.A. Martin, A. Solla, M.A. Coimbra, L. Gil, Metabolic fingerprinting allows discrimination between *Ulmus pumila* and *U. minor*, and between U. Minor clones of different susceptibility to Dutch elm disease, For. Pathol. 38 (2008) 244–256, https://doi.org/10.1111/j.1439-0329.2007.00542.x.
[31] G.F. Antonova, V.V. Stasova, Seasonal development of phloem in scots pine stems, Russ. J. Dev. Biol. 37 (2006) 306–320, https://doi.org/10.1134/S1062360406050043.
[32] X. Moreira, R. Zas, L. Sampedro, Differential allocation of constitutive and induced chemical defenses in pine tree juveniles: a test of the optimal defense theory, PLoS One 7 (2012) 1–8, https://doi.org/10.1371/journal.pone.0034006.
[33] K.K. Pandey, K.S. Theagarajan, Analysis of wood surfaces and ground wood by diffuse reflectance (DRIFT) and photoacoustic (PAS) Fourier transform infrared spectroscopic techniques, Holz Als Roh - Und Werkst. 55 (1997) 383–390, https://doi.org/10.1007/s001070050251.
[34] K.K. Pandey, A.J. Pitman, FTIR studies of the changes in wood chemistry following decay by brown-rot and white-rot fungi, Int. Biodeterior. Biodegrad. 52 (2003) 151–160, https://doi.org/10.1016/S0964-8305(03)00052-0.
[35] M.C.D.B. Cardinali, P.R. Villas Boas, D.M.B.P. Milori, E.J. Ferreira, M.F.E. Silva, M.A. MacHado, B.S. Bellete, M.F.D.G.F. Da Silva, Infrared spectroscopy: A potential tool in huanglongbing and citrus variegated chlorosis diagnosis, Talanta 91 (2012) 1–6, https://doi.org/10.1016/j.talanta.2012.01.008.
[36] M. Abdallah, H.M. Kamal, A. Abdrabou, Investigation, preservation and restoration processes of an Ancient Egyptian wooden offering table, Int. J. Conserv. Sci. 7 (2017) 1047–1064.
[37] M. Karim, M.G. Daryaei, J. Torkaman, R. Oladi, M.A.T. Ghanbary, E. Bari, N. Yilgor, Natural decomposition of hornbeam wood decayed by the white rot fungus Trametes versicolor, An. Acad. Bras. Cienc. 89 (2017) 2647–2655, https://doi.org/10.1016/j.surfcoat.2018.04.062.
[38] K. Fackler, M. Schwanninger, How spectroscopy and microspectroscopy of degraded wood contribute to understand fungal wood decay, Appl. Microbiol. Biotechnol. 96 (2012) 587–599, https://doi.org/10.1007/s00253-012-4369-5.
[39] M. Danielsson, K. Lundén, M. Elfstrand, J. Hu, T. Zhao, J. Arnerup, K. Ihrmark, G. Swedjemark, A.-K. Borg-Karlson, J. Stenlid, Chemical and transcriptional responses of Norway spruce genotypes with different susceptibility to *Heterobasidion* spp. Infection, BMC Plant Biol. 11 (2011) 154, https://doi.org/10.1186/1471-2229-11-154.
[40] A. Kovalchuk, S. Kerí, A.O. Oghenekaro, E. Jaber, T. Raffaello, F.O. Asiegbu, Antimicrobial defenses and resistance in forest trees: challenges and perspectives in a genomic era, Annu. Rev. Phytopathol. 51 (2013) 221–244, https://doi.org/10.1146/annurev-phyto-082712-102307.
[41] J. Arnerup, M. Nemesio-Gorriz, K. Lundén, F.O. Asiegbu, J. Stenlid, M. Elfstrand, The primary module in Norway spruce defence signalling against *H annosum* s.l. Seems to be jasmonate-mediated signalling without antagonism of salicylate-mediated signalling, Planta 237 (2013) 1037–1045, https://doi.org/10.1007/s00425-012-1822-8.
[42] I. Kaplan, R. Halitschke, A. Kessler, S. Sardanelli, R.F. Denno, Constitutive and induced defences to herbivory in above- and belowground plant tissues, Ecology 89 (2008) 392–406, https://doi.org/10.1890/07-0471.1.
[43] A.R. War, M.G. Paulraj, T. Ahmad, A.A. Buhroo, B. Hussain, S. Ignacimuthu, H.C. Sharma, Mechanisms of plant defense against insect herbivores, Plant Signal. Behav. 7 (2012) 1306–1320, https://doi.org/10.4161/psb.21663.
[44] C.P. Constabel, K. Yoshida, V. Walker, Diverse ecological roles of plant tannins: plant defense and beyond, recent adv, Polyphen. Res. 4 (2014) 115–142, https://doi.org/10.1002/9781118329634.ch5.
[45] F. He, Q.H. Pan, Y. Shi, C.Q. Duan, Chemical synthesis of proanthocyanidins in vitro and their reactions in aging wines, Molecules 13 (2008) 3007–3032, https://doi.org/10.3390/molecules13123007.
[46] M. Schwanninger, J.C. Rodrigues, N. Gierlinger, B. Hinterstoisser, Determination of lignin content in Norway spruce wood by Fourier transformed near infrared spectroscopy and partial least squares regression. Part 1: wavenumber selection and evaluation of the selected range, J. Near Infrared Spectrosc. 19 (2011) 319–329, https://doi.org/10.1255/jnirs.944.
[47] G. Zhou, G. Taylor, A. Polle, FTIR-ATR-based prediction and modelling of lignin and energy contents reveals independent intra-specific variation of these traits in bioenergy poplars, Plant Methods 7 (2011) 9, https://doi.org/10.1186/1746-4811-7-9.
[48] E.C. Leong, D.C. Burcham, Y.K. Fong, A purposeful classification of tree decay detection tools, Arboric. J. 34 (2012) 91–115, https://doi.org/10.1080/03071375.2012.701430.